Title	EM-TCAD solving from 0-100 THz: a new implementation of an electromagnetic solver
Author(s)	Chen, Q; Schoenmaker, W; Banagaaya, N; Schilders, W; Wong, N
Citation	The 41st European Solid-State Device Research Conference (ESSDERC) and the 37th European Solid-State Circuits Conference (ESSCIRC), Helsinki, Finland, 12-16 September 2011. In European Conference on Solid-State Device Research Proceedings, 2011, p. 351-354
Issued Date	2011
URL	http://hdl.handle.net/10722/158748
Rights	European Conference on Solid-State Device Research Proceedings. Copyright © IEEE.

EM-TCAD Solving from 0-100 THz: A New Implementation of an Electromagnetic Solver

Quan Chen
Department of Computer Science and Engineering
University of California, San Diego, USA
Email: q1chen@ucsd.edu

Wim Schoenmaker
MAGWEL NV
Leuven, Belgium
Email: wim@magwel.com

Nico Banagaaya
TU Eindhoven
Eindhoven, The Netherlands
Email: n.banagaaya@tue.nl

Wil Schilders
TU Eindhoven
Eindhoven, The Netherlands
Email: w.h.a.schilders@tue.nl

Ngai Wong
Department of Electrical and Electronic Engineering
University of Hong Kong, Hong Kong
Email: nwong@eee.hku.hk

***Abstract*— This paper deals with reformulating the electromagnetic field equations for a combined EM and TCAD approach in such a way that both extreme high and low frequencies can be solved. The importance of the method is found in eliminating the need for direct solvers which are restricted in application to very large systems. We elaborate on the numerical recipe for finding field solutions using the generic TCAD procedure based on the Newton-Raphson method combined with iterative solvers.**

I. Introduction

In a recent paper [1] we have presented a transformation of the electromagnetic field drift-diffusion system such that the resulting equations become much more attractive to solve at extreme high frequencies. As was demonstrated in our earlier work the incorporation of magnetic effects into the semi-conductor equations demands that these effects are represented by the vector potential [2], [3]. The key argument is that the Poisson potential is required to obtain the carrier densities. In [1] we have named the resulting set of equations the AV system or AV formulation. It consists of the drift-diffusion equations completed with the Maxwell equations in the potential formulation. After having discretized this system of equations and applying them to industrial design problems [4], we experienced a dramatic drop in convergence behavior if the frequencies go up. Depending on the structure under consideration, iterative solving schemes fail for frequencies above ∼50-200 GHz. In [1] we have identified the causes for this convergence failure and proposed a remedy for it. The purpose of this contribution is two-fold: (1) We present the proposed remedy in a wider perspective. (2) We report on the learning cycles for setting up a successful series of linear solving settings to arrive at good convergence of the newly proposed formulation.

II. From AV to EV

As was shown in [1] the central observation for explaining the deterioration of solving the AV system at high frequencies is that the Poisson system (V) couples to the magnetic system represented by $\mathbf{A}$ with a term proportional to the frequency, ω and the conductance σ in metallic domains or $q\mu_{\rm n}n$ or $q\mu_{\rm p}p$ in n-doped or p-doped regions respectively. This coupling destroys the diagonal dominance of the Newton-Raphson matrices in such a way that at sufficient high frequencies no suitable preconditioner can be found despite using highly sophisticated permutation algorithms [5]. The cure of the convergence failure problem is to apply a transformation of variables in such a way that the coupling is removed. Starting from the AV formulation summarized in equations (1-8) with ξ a slider between the Coulomb gauge ($\xi = 0$) and the Lorenz gauge ($\xi = 1$)

$$\nabla \cdot (\epsilon \mathbf{E}) - \rho = 0 \quad (1)$$

$$\nabla \cdot \mathbf{J}_{\rm metal} + {\rm j}\omega\rho = 0,\ \mathbf{J}_{\rm metal} = \sigma\mathbf{E} \quad (2)$$

$$\nabla \cdot \mathbf{J}_{\rm p} + {\rm j}\omega qp + q(R-G) = 0,\ \mathbf{J}_{\rm p} = q\mu_{\rm p}p\mathbf{E} - qD_{\rm p}\nabla p \quad (3)$$

$$\nabla \cdot \mathbf{J}_{\rm n} - {\rm j}\omega qn - q(R-G) = 0,\ \mathbf{J}_{\rm n} = q\mu_{\rm n}n\mathbf{E} + qD_{\rm p}\nabla n \quad (4)$$

$$\nabla \times \left(\frac{1}{\mu}\nabla \times \mathbf{A}\right) - \mathbf{J}_{\rm c} - {\rm j}\omega\epsilon\mathbf{E} = 0 \quad (5)$$

$$\nabla \cdot \mathbf{A} + {\rm j}\omega\mu\epsilon\xi V = 0 \quad (6)$$

$$\mathbf{E} = -\nabla V - {\rm j}\omega\mathbf{A} \quad (7)$$

$$p = n_{\rm i}\exp\left(\phi_{\rm p} - V\right),\ n = n_{\rm i}\exp\left(V - \phi_{\rm n}\right) \quad (8)$$

we rewrite this system of equations using (7) by performing a transformation of variables $\mathbf{A} = \frac{\rm j}{\omega}\left(\mathbf{E} + \nabla V\right)$. Of course $\mathbf{E}$ is the electric field but the point is that starting from six field degrees of freedom $\{V, \phi_{\rm p}, \phi_{\rm n}, A_x, A_y, A_z\}$ we transform to six different field degrees of freedom $\{V, \phi_{\rm p}, \phi_{\rm n}, E_x, E_y, E_z\}$. The system of equations (1-8) gets adapted for (5) and (6) leading to

$$\nabla \times \left(\frac{1}{\mu}\nabla \times \mathbf{E}\right) - \mathbf{J}_{\rm c} - {\rm j}\omega\epsilon\mathbf{E} = 0 \quad (9)$$

$$\nabla \cdot \mathbf{E} + \nabla^2 V + {\rm j}\omega\xi V = 0 \quad (10)$$

In [1] we have named the system of equations (1-4) together with (9-10), the EV system or EV formulation. Before entering

978-1-4577-0708-7/11/$26.00 ©2011 IEEE

the details of solving this system we note that the EV formulation resembles the usual Maxwell system in the frequency domain using $\mathbf{B} = \frac{\mathrm{j}}{\omega}\nabla \times \mathbf{E}$. Thus the question arises why there is a voltage variable V left over at all. Apart from the evident answer that the transformation of variables does not "transform away" degrees of freedom, there is the observation that (9) contains the singular operation $\nabla \times \nabla$ that needs regularization by an additional constraint, e.g., equation (10). Finally, it is indeed possible to avoid usage of the voltage variable V completely. In order to achieve this one must refrain from the Coulomb or Lorenz gauge (6, 10) and select the *temporal gauge* $V = 0$. However, as was argued in the introduction, in this gauge it becomes very awkward (if not impossible) to compute carrier densities in semiconductors.

III. Discretization

Although the term $\nabla \times (\frac{1}{\mu}\nabla \times \mathbf{E})$ in (9) is singular (non-invertible), when combined with $\mathbf{J}_{\mathrm{total}} = (\sigma + \mathrm{j}\epsilon\omega)\mathbf{E}$, it is regular for $\omega \neq 0$ and $\sigma \neq 0$ and/or $\epsilon \neq 0$. Yet, we can improve its iterative convergence behavior substantially by making it more Laplacian-alike by subtracting $\nabla(\frac{1}{\mu}\nabla \cdot \mathbf{E})$. For constant permeability we may subtract the divergence of (10) from (9) without altering the solution. The resulting equation is

$$\nabla \times \left(\frac{1}{\mu}\nabla \times \mathbf{E}\right) - \nabla\left[\nabla \cdot \mathbf{E} + \nabla^2 V + \mathrm{j}\omega\xi V\right] - \mathbf{J}_{\mathrm{total}} = 0 \tag{11}$$

Equation (11) is the starting point for the discretization of the EV system. The discretization is done fully analogous to the discretization of the AV system in [2]. This approach requires that a grid variable E_k is assigned to every link in the computational grid representing the projection of the electric field in the direction of that link. In regions with constant permittivity and zero charge we obtain from (1) that $\nabla \cdot \mathbf{E} = 0$ and therefore in those regions we also could use

$$\nabla \times \left(\frac{1}{\mu}\nabla \times \mathbf{E}\right) + \nabla\left(\nabla \cdot \mathbf{E}\right) - \mathbf{J}_{\mathrm{total}} = 0 \tag{12}$$

When addressing structures that contain semiconducting regions, equations (3) and (4) are part of the system of equations that need to be solved. With metals included equation (2) can be added to make the solution satisfy current continuity everywhere. Acting with the divergence on (11) and (12) implies that

$$\nabla^2\left[\nabla \cdot \mathbf{E} + \nabla^2 V + \mathrm{j}\omega\xi V\right] = 0 \tag{13}$$

$$\nabla^2\left[\nabla \cdot \mathbf{E}\right] = 0 \tag{14}$$

The following theorem plays an important role to complete the discretization:

Theorem: *If* $\nabla^2 f = 0$ *for some domain* Ω *and* $f = 0$ *at the boundary of the domain* $\partial\Omega$*, then* $f = 0$ *everywhere inside* Ω*.*

Thus the discretization requires that (11) or (12) is imposed for the surface of the simulation domain and as a consequence the gauge condition and/or Gauss' law is obtained everywhere when solving (3, 4) and (11) or (12). In this way the redundancy in the formulation of the full system of equations is avoided [1], [6]. It is interesting to note that the argumentation can be inverted: solving the gauge condition or Gauss' law everywhere as well as (11, 12), guarantees current continuity. However, although such analytic observations can be easily deduced, their numerical benefits still need to be shown. In our numerical experiments we have found that the first route is the preferred one, i.e. imposing current continuity explicitly is a more robust scheme than imposing the gauge condition or Gauss' law explicitly.

1) Simplified EV schemes: In the numerical experiments discussed below, we have marked the results that are based on the approach using Gauss' law, e.g. equation (12) by the label 'EV-Gauss'. The results that are obtained using the gauge conditions, e.g. equation (11) is based on older work at MAGWEL and is labeled as 'EV-Magwel'. An interest line of reasoning, inspired by the universal validity of Gauss' law is to apply it in the gauge condition (10) in regions of zero charge and constant permittivity, i.e. inside metals and insulators :

$$\nabla^2 V + \mathrm{j}\omega\xi V = 0 \tag{15}$$

This route was originally explored by the authors (Chen and Schoenmaker). Its appealing feature is that large blocks of entries in the Newton matrix originating from EV mixing empty, thereby speeding up the (iterative) solving considerably. In the numerical experiments discussed below we have marked the corresponding results by the label 'EV-Chen'. Thus the resulting system is based on equation (12) and (15) in charge-free regions and keep equation (12) elsewhere, i.e. at interfaces. It should be emphasized that this approach is approximate since it modifies the system of equations in such a way that their physical content changes. This can be understood from the fact that acting with the divergence on the Maxwell-Ampere equation (12) leads to $\nabla^2(\nabla \cdot \mathbf{E}) - \mathrm{j}\mu\omega(\sigma + \mathrm{j}\epsilon)(\nabla \cdot \mathbf{E}) = 0$ or $\nabla^2 f + kf = 0$ for $f = \nabla \cdot \mathbf{E}$ and $k \neq 0$ constant and therefore the theorem is not applicable. Indeed the numerical solutions that were obtained using this approach show deviations from the physical correct ones, meaning that non-zero values for f have been mixed in. The deviations are in some cases rather small and therefore the method can still generate valuable results. However, so far we have no general guidelines when the method is sufficiently accurate.

IV. Combination of AV and EV Solvers

The AV and EV solvers have a complementary working range. The AV solver works well at low and medium frequencies ($0 - 50$GHz) whereas the EV solver behaves competent at high frequencies (> 50GHz). Combining the merits of the two solvers will enable a true wide-band EM-TCAD co-simulator. The following pseudo-code algorithm provides a convenient upgrading of the AV solver to include an EV solver applying a 4-step solution strategy:

1) Map $\mathbf{A} - V$ variables onto $\mathbf{E} - V$ variables via $\mathbf{A} = \frac{\mathrm{j}}{\omega\epsilon}(\mathbf{E} + \nabla V)$.

2) Apply the EV solver to compute the update vector $[\Delta V, \Delta \mathbf{E}]^T$ in Newton iteration.
3) Map $[\Delta V, \Delta \mathbf{E}]^T$ onto $[\Delta V, \Delta \mathbf{A}]^T$
4) Update the AV system.

Using this approach, the data structure in the original AV solver is unaltered and the switching between the AV and EV solvers is easy to realize.

V. Numerical Experiments

In this section we present a numerical experiment to demonstrate the characteristics of the AV and EV schemes. Many more examples exist but the generic trend is similar to the one shown here. We focus on the eigenvalues and condition numbers of the Newton-Raphson matrices. A simple square inductor with 3.5 windings is used as illustrated in Fig. 1. We applied a simple structured mesh since the focus is here on testing the qualities of the linear system. In Fig. 2 we

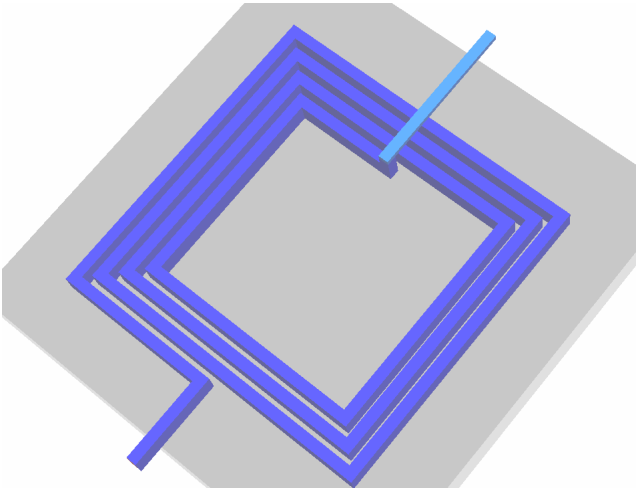

Fig. 1. Lay out of an integrated inductor problem.

plot the solution for the potential field V in the inductor plane computed using the AV scheme, whereas in Fig. 3 we show the potential field computed according to the EV scheme. Fig. 4 shows the magnitude of the electric field computed using the AV scheme and Fig. 5 shows the same variable using the EV scheme. The plots are pair wise identical demonstrating that the transformation from the AV to EV system has no effect on the solution as it should.

In Fig. 6 the condition number vs. the frequency is shown for the various solution strategies. As is observed, the three EV versions have very large condition numbers at low frequency which drop and the AV solver has the smallest condition number at low frequency which gradually goes up. Around 50 GHz the curves do cross meaning that from then onwards it is more favorable to use EV solving.

In order to obtain a better understanding of the patterns that are seen in Fig. 6 (we observed similar patterns in many different structure setups) we have zoom in at the eigenvalues of the Newton-Raphson matrices. For the AV solver we find

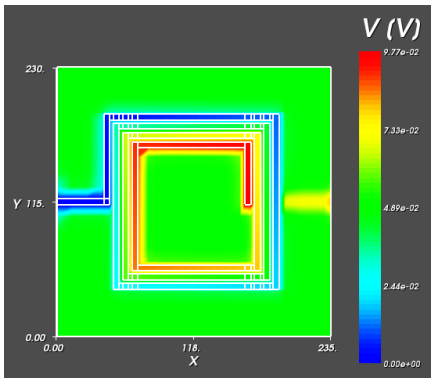

Fig. 2. Voltage in the inductor plane at 10GHz using the AV solver.

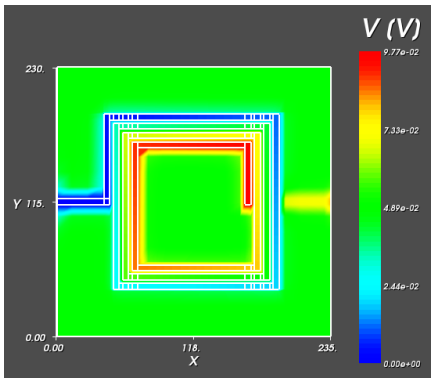

Fig. 3. Voltage in the inductor plane at 10GHz using the EV Guass solver.

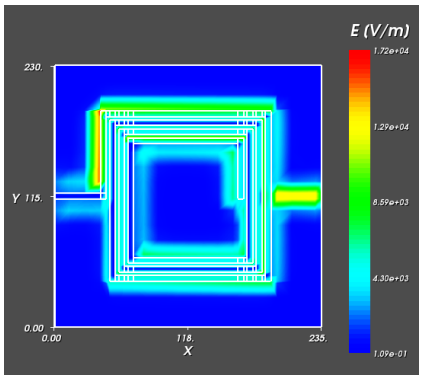

Fig. 4. Magnitude of the electric field in the inductor plane at 10GHz using the AV solver.

that the real part of the smallest (in magnitude) eigenvalue as a function of frequency is $\lambda_0(\omega) \sim \text{const}$ and the constant of order 10^{-2}. On the other hand the smallest eigenvalue for the EV solver behaves as $\lambda_0(\omega) \sim \text{const}'/\omega$ where const$'$ is also of order 10^{-2}. This explains why EV solving becomes difficult at low frequencies. On the other hand the modulus largest eigenvalues are constant for both cases. However, for the AV solver the value is $O(10^{10})$, whereas for the EV solver the value is $O(10^6)$. Since the condition number can be seen as a measure for the ratio of the smallest and the largest

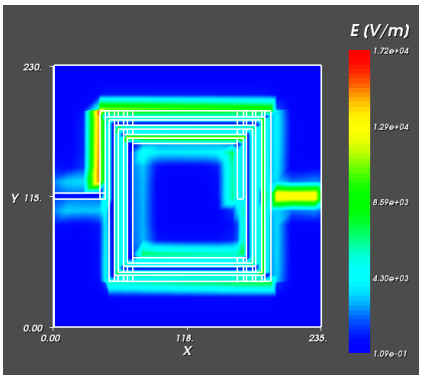

Fig. 5. Magnitude of the electric field in the inductor plane at 10GHz using the EV Guass solver.

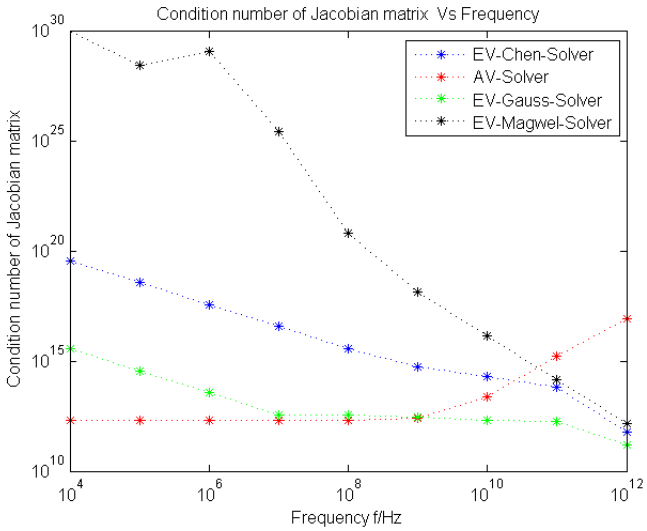

Fig. 6. condition number Vs frequency for the integrated inductor problem.

f (Hz)	**E**-V-Magwel	**E**-V-Chen	**E**-V-Gauss	**A**-V
10^4	1.00×10^{30}	3.82×10^{19}	3.67×10^{15}	1.98×10^{12}
10^5	2.87×10^{28}	3.82×10^{18}	3.67×10^{14}	1.98×10^{12}
10^6	1.26×10^{29}	3.82×10^{17}	3.67×10^{13}	1.98×10^{12}
10^7	2.9×10^{25}	3.82×10^{16}	3.67×10^{12}	1.99×10^{12}
10^8	6.72×10^{20}	3.85×10^{15}	3.43×10^{12}	2.05×10^{12}
10^9	1.47×10^{18}	5.28×10^{14}	2.91×10^{12}	2.59×10^{12}
10^{10}	1.47×10^{16}	2.12×10^{14}	2.02×10^{12}	2.42×10^{13}
10^{11}	1.47×10^{14}	6.56×10^{13}	1.88×10^{12}	1.63×10^{15}
10^{12}	1.48×10^{12}	5.75×10^{11}	1.60×10^{11}	8.38×10^{16}

TABLE I
CONDITION NUMBERS OF THE **A**-V AND **E**-V-SOLVERS.

eigenvalue we identified the cause of the pattern observed in Fig. 6. Moreover, the repetitive character of the pattern allows to identify a switching point in the solver between the AV and EV approach. This point is located around ∼50 GHz.

2) Best practices for iterative solving: We end the section with reporting on our experience of solving the AV and EV systems using iterative solvers. As far as the AV system is concerned the most robust approach that we identified applies matrix row/column permutation using the method of Duff and Koster [5]. Its purpose is to make the diagonal as dominant as possible. Next a standard procedure of incomplete LU decomposition is applied followed by a linear solver such as BiCGStab [8]. For the EV system, we have a different starting point: note that in the EV Gauss formulation it is the Maxwell-Ampere equation that implicitly determines V and Gauss' law (14) is generating entries in the Newton-Raphson matrix which are fully off-diagonal. It turns out that the method of [5] does not lead to a good pre-ordering of the linear system. However, with the approximate minimum degree (AMD) method and in particular, the variant COLAMD [9], the permuted system is suitable for iterative solving. The more robust choice of linear solver is CGS [10].

VI. CONCLUSION

In this paper we presented a new approach to solve EM-TCAD problems. It is based on the desire to keep the variable $V(\mathbf{x})$ in the formulation such that a straightforward mapping on the Kirchhoff variables V_{node} is preserved. Whereas this approach leads naturally to AV solving, it suffers from convergence issues at high frequencies. We have given a system of equations that becomes attractive to solve at extreme high frequencies. Combining both methods allows us to scan the full frequency range from 0 to 100 THz.

ACKNOWLEDGMENT

This work is partly funded by the EU project ICESTARS (IST-214911) and the MEDEA+ project COSIP (IWT) as well as the Hong Kong Research Grants Council under Projects HKU 717407E and 718509E of the University Research Committee of The University of Hong Kong.

REFERENCES

[1] Q. Chen, W. Schoenmaker, P. Meuris and N. Wong, "An effective formulation of coupled electromagnetic-TCAD simulation for extremely high frequency onwards," *IEEE Trans. Comput.-Aided Design*, to appear.
[2] P. Meuris and W.Schoenmaker "Strategy for electromagnetic interconnect modeling," *IEEE Trans. Comput.-Aided Design*, 20(6), 753-762, Jun 2001.
[3] W. Schoenmaker and P. Meuris, "Electromagnetic interconnects and passives modeling: software implementation issues," *IEEE Trans. Comput.-Aided Design*, 21(5), 534-543, May 2002.
[4] W. Schoenmaker, P. Meuris, W. Pflanzl and A. Steinmair, *Scientific Computing in Electrical Engineering SCEE2008*, Eds. J. Roos and L. Costa, Springer Verlag Berlin Heidelberg 2010
[5] I. Duff and J. Koster "On algorithms for permuting large entries to the diagonal of a sparse matrix," *SIAM J MATRIX ANAL APPL* , 22(4), 973-996, 2001
[6] P. Endes "Underteminacy and Redundance in Maxwell's Equations"*Electronic Journal of Theoretical Phys. EJTP 6*, 135-166, 2009
[7] Nicodemus Banagaaya, "The EV-formulation and an investigation of eigenvalues for electromagnetic problems," *Master Thesis*. TU Eindhoven, The Netherlands, August 2010
[8] H. van der Vorst "Bi-CGSTAB, A fast and smoothly converging variant of Bi-CG for the solution of nonsymmetric linear systems" *SIAM J. Sci. Statist. Comput* 13, 631-644, 1989
[9] T. A. Davis, J. R. Gilbert, S. Larimore, E. Ng, "Algorithm 836: COLAMD, an approximate column minimum degree ordering algorithm " *ACM Transactions on Mathematical Software* vol. 30, no. 3., pp. 377-380, 2004
[10] P. Sonneveld "CGS, a fast Lanczos-type solver for nonsymmetric linear systems" *SIAM J. Sci. Statist. Comput.* 10, 36-52, 1989